Journal of Cerebral Blood Flow & Metabolism (2009) 29, 976–986

www.jcbfm.com

Pathway-specific variations in neurovascular and neurometabolic coupling in rat primary somatosensory cortex

Pia Enager[1,5], Henning Piilgaard[1,5], Nikolas Offenhauser[1,2], Ara Kocharyan[3], Priscilla Fernandes[3], Edith Hamel[3,6] and Martin Lauritzen[1,4,6]

[1]*Department of Neuroscience and Pharmacology, The Panum Institute, University of Copenhagen, Blegdamsvej , Copenhagen N, Denmark;* [2]*Department of Experimental Neurology, Charité Universitätsmedizin Berlin, Berlin, Germany;* [3]*Department of Neurology and Neurosurgery, Montreal Neurological Institute, McGill University, Montréal, Quebec, Canada;* [4]*Department of Clinical Neurophysiology, Glostrup Hospital, Glostrup, Denmark*

Functional neuroimaging signals are generated, in part, by increases in cerebral blood flow (CBF) evoked by mediators, such as nitric oxide and arachidonic acid derivatives that are released in response to increased neurotransmission. However, it is unknown whether the vascular and metabolic responses within a given brain area differ when local neuronal activity is evoked by an activity in the distinct neuronal networks. In this study we assessed, for the first time, the differences in neuronal responses and changes in CBF and oxygen consumption that are evoked after the activation of two different inputs to a single cortical area. We show that, for a given level of glutamatergic synaptic activity, corticocortical and thalamocortical inputs evoked activity in pyramidal cells and different classes of interneurons, and produced different changes in oxygen consumption and CBF. Furthermore, increases in stimulation intensities either turned off or activated additional classes of inhibitory interneurons immunoreactive for different vasoactive molecules, which may contribute to increases in CBF. Our data imply that for a given cortical area, the amplitude of vascular signals will depend critically on the type of input, and that a positive blood oxygen level-dependent (BOLD) signal may be a consequence of the activation of both pyramidal cells and inhibitory interneurons.
Journal of Cerebral Blood Flow & Metabolism (2009) **29,** 976–986; doi:10.1038/jcbfm.2009.23; published online 1 April 2009

Keywords: blood flow; glutamate; interneurons; oxygen tension; synaptic activity; whisker barrel

Introduction

Functional neuroimaging, such as positron emission tomography and functional magnetic resonance imaging (fMRI) is based on the coupling between neuronal activity and the accompanying changes in cerebral blood flow (CBF) and metabolism (Sokoloff, 1999; Lauritzen, 2005). Increases in the intensity of functional brain imaging signals indicate increases in neuronal activity. A number of studies using the 2-deoxyglucose method have shown that the functional activation of energy metabolism that is localized to the terminal synaptic zones of the activated pathway, is proportional to the spike frequency of the afferent input to these terminal zones of the activated pathway, and is localized to the synapses but not in the postsynaptic cell bodies even though these cell bodies must have been activated as evidenced by alterations in energy metabolism in the further projection zones of these postsynaptic neurons (Schwartz *et al*, 1979; Kadekaro *et al*, 1985) (Sokoloff, 1999; Raichle and Mintun, 2006). Therefore, even if increases in spiking activity of targeted neurons do correlate with the amplitude of BOLD (blood oxygen level-dependent) signals in functional magnetic resonance imaging studies, this correlation is not an cause–effect relationship, and the mechanisms that generate the signals relate to the dendritic processing of incoming synaptic inputs rather than to the production of spikes (Logothetis *et al*, 2001) (Lauritzen, 2005). The objective of our study was to explore the cellular mechanisms of

Correspondence: Dr M Lauritzen, Department of Clinical Neurophysiology, Glostrup Hospital & University of Copenhagen, DK-2600 Glostrup, Denmark.
E-mail: mlauritz@mfi.ku.dk
[5]These authors contributed equally to this work.
[6]These authors contributed equally to this work.
Received 14 November 2008; revised 23 February 2009; accepted 27 February 2009; published online 1 April 2009

activity-dependent increases in CBF and cerebral metabolic rate of oxygen ($CMRO_2$) in two networks targeting the same small locus of the cortex, in which the activated neuronal cell types were identified by immunocytohistochemistry.

We stimulated the infraorbital (IO) nerve or transcallosal (TC) afferents that activate both stellate and pyramidal cells, as well as interneurons through glutamate release and activation of alpha-amino-3 hydroxy-5 methyl-4 isoxazole proprionic acid (AMPA) and N-methyl D-aspatate (NMDA) receptors (Armstrong-James *et al*, 1993; Conti and Manzoni, 1994; Nielsen and Lauritzen, 2001; Hoffmeyer *et al*, 2007). Infraorbital stimulation excites thalamocortical neurons in layer IV of the barrel cortex followed by an activation of neurons in layers II and III and, to a lesser extent, in the intermingled septa (Woolsey and Rovainen, 1991; Shepherd *et al*, 2005). In contrast, TC stimulation excites primarily septa-located neurons on the contralateral side in layers III and V followed by an activation in layer II (Wise and Jones, 1976; Olavarria *et al*, 1984; Shepherd *et al*, 2005; Petreanu *et al*, 2007). Double immunocytochemistry identified the neuronal cell types that were stimulated, and their contents of vasoactive intestinal polypeptide (VIP), or enzymes capable of producing or releasing vasodilators (cyclooxygenase-2, COX-2; nitric oxide synthase, NOS) or generating their synthesis in neighboring perivascular astrocytes. We report that increases in CBF and $CMRO_2$ were greater when evoked by incoming cortico-cortical afferents than by thalamocortical afferents for the same level of synaptic activity. Furthermore, interneurons with different contents of vasodilators were activated at low and high stimulation frequencies. We suggest that the response amplitudes of vascular and metabolic signals reflect distinct properties of activated neurons in addition to the magnitude of the evoked synaptic activity, and that activation of both pyramidal cells and inhibitory interneurons may produce a positive BOLD response. Our study specifies the dependence of CBF and energy usage on pathway and incoming synaptic inputs, and may help to define the ability of functional imaging to detect changes in neural activity.

Materials and methods

All experiments were in full compliance with the guidelines set forth in the European Council's Convention for the Protection of Vertebrate Animals Used for Experimental and other Scientific Purposes and were approved by the Danish National Ethics Committee. Forty-one male Wistar rats (350 ± 10 g) were anesthetized with isoflurane (induction: 5% and surgery: 2%) while ventilated with O_2 and air (Hoffmeyer *et al*, 2007). The trachea was cannulated for mechanical ventilation, and small catheters were placed into the left femoral artery and vein, which were continuously perfused with physiological saline. Continuous monitoring of arterial blood pressure and hourly blood samples of arterial pH, pO_2, and pCO_2 assured the maintenance of basic physiological parameters. Body temperature was maintained at 36°C to 37°C using a custom-made heating pad. The head was fixed in a stereotaxic frame. Depending on protocol, one (IO) or two (TC), craniotomies were performed over homologous regions of the somatosensory cortex. After surgery, the anesthesia was changed to α-chloralose HBC complex, which was dissolved in saline (0.5 g/mL) (bolus: 1.6 mL/kg intravenously; continuous infusion: 1.1 mL/kg per h intravenously), which would correspond to a dose of initial bolus (1.6 mL/kg × 51.5 mg/mL) of 82.4 mg/kg and continuous infusion (1.1 mL/kg per h × 51.5 mg/mL) of 56.7 mg/kg per h, if using α-chloralose. The level of anesthesia was checked by observing arterial blood pressure during stimulation and by tail pinch.

Stimulation Protocol

In 10 experiments, the ramus infraorbitalis (IO) of the left trigeminal nerve was stimulated by a set of custom-made electrodes inserted percutaneously. The cathode was positioned at the hiatus infraorbitalis and the anode was inserted into the masticatory muscles (Figures 1A and 1C) (Nielsen and Lauritzen, 2001). In other six experiments, a coated bipolar stainless-steel electrode (SNEX 200, contact separation: 0.25 mm; RMI, Woodland Hills, CA, USA) was lowered 0.5 mm into the left sensory cortex, 3.0 mm posterior to the bregma, and 6.0 mm lateral to the midline using stereotactic instruments for TC stimulation (Hoffmeyer *et al*, 2007). The site used for the stimulation of TC fibers was selected as the homologous cortical region contralateral to the locus, at which the responses were recorded for IO stimulation (Figures 1C and 1D), i.e., at coordinates −3, 6 on the contralateral side. To prevent the elicitation of cortical spreading depression (CSD) on the stimulated side, we applied the NMDA receptor antagonist, MK801 (1 mmol/L), to the stimulated cortex (Hoffmeyer *et al*, 2007). For both IO and TC stimulation, we used direct current stimulation (ISOflex; A.M.P.I., Jerusalem, Israel) given as square wave pulses (0.1 ms, 1.5 mA) at 0.25, 0.5, 1, 2, 4, 6, 30, and 40 Hz in trains lasting for 4 secs. Each frequency was run three times with interstimulus intervals of 0.5 to 1.5 min, depending on the stimulation frequency for allowing both the electroencephalogram (EEG) and the basal CBF to return to stable baseline values between stimulations.

Double Immunocytochemistry for Identification of Activated Cortical Neurons

Rats were stimulated either under acute or chronic conditions; the latter group being craniotomized 1 week before stimulation. Only one craniotomy was performed over the left cortex when TC stimulation was carried out, whereas the right skull was kept intact, and both the right and the left skull was intact during IO stimulation experiments. Acute rats received left IO (4 and 20 Hz, $n = 3$ to 4 rats per group) or TC (4 and 20 Hz, $n = 4$ rats per group) stimulation for 20 mins. In chronic experiments, rats received high-frequency (30 Hz) left IO ($n = 1$ sham and 3 stimulated) or TC ($n = 2$ sham and 4 stimulated) stimulation for 20 mins. After stimulation, rats were kept

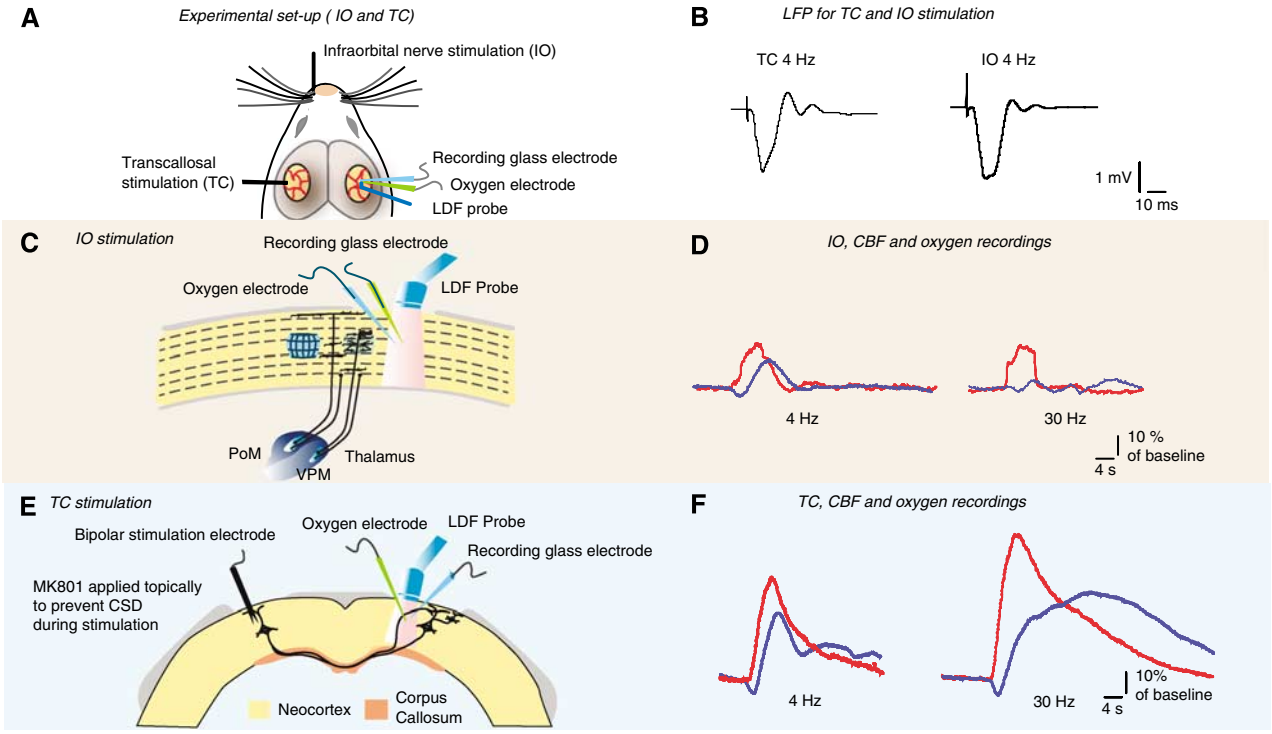

Figure 1 Experimental setup. (**A**) Schematic drawing of experimental setup. Depending on the protocol, one (infraorbital, IO) or two (transcallosal, TC) craniotomies were performed over homologous regions of the somatosensory cortex; stimulation was on the left side and registration on the right side. IO nerve stimulation: The ramus infraorbitalis of the left trigeminal nerve was stimulated by custom-made electrodes inserted percutaneously. TC stimulation: A bipolar stimulation electrode was positioned in the left primary somatosensory cortex 3.0 mm posterior to the bregma and 6.0 mm lateral to the midline. In the right somatosensory cortex, electrophysiological recordings of local field potentials (LFPs) were performed by a glass microelectrode. A modified Clark-type oxygen electrode was placed at the same depth for simultaneous recordings of changes in tissue oxygen tension (tpO_2). CBF was recorded by a LDF probe, located close to the two electrodes positioned at 0.3 to 0.5 mm above the pial surface. (**B**) Averaged LFP recordings at 4 Hz for both TC ($n = 6$) and IO stimulation ($n = 10$). Infraorbital stimulation is further illustrated in (**C**), which shows that the excitatory input to pyramidal cells in layer IV in the right primary somatosensory cortex (SI) is through the VPM part of the thalamus. (**D**) Depicts CBF (red) and tpO_2 (blue) responses at 4 and 30 Hz after infraorbital nerve stimulation ($n = 10$). The TC setup is illustrated in (**E**). TC fibers project to and synapse in layers II/III and V in the homologue region on the contralateral side. (**F**) Depicts CBF (red) and tpO_2 (blue) responses at 4 and 30 Hz after TC stimulation ($n = 6$).

stable in the setup for 1 h (to allow c-Fos protein expression) before perfusion through the ascending aorta with 4.0% ice-cold paraformaldehyde (500 ml in a 0.1 mol/L phosphate buffer solution, pH 7.4). Brains were post-fixed, cryoprotected, frozen in isopentane, and free-floating coronal sections (25 μm thick) were obtained as described earlier (Kocharyan *et al*, 2008).To visualize the locus of cortical activation, the sections were first incubated overnight for c-Fos immunocytochemistry with a rabbit anti-c-Fos antibody (1:15,000; Oncogene, San Diego, CA, USA) revealed with a biotinylated secondary antibody detected using the SG reagent (SK-4700, Vector Labs, Burlingame, CA, USA, blue–grey precipitate). The identity of the activated cells was then determined by double immunostaining for c-Fos and markers of a subset of pyramidal cells— COX-2—or the three main subtypes of gamma-aminobutyric acid (GABA) interneurons namely, somatostatin (SOM)-, VIP-, or parvalbumin (PV)-containing cells (Kubota *et al*, 1994). As NOS interneurons represent a subpopulation of SOM interneurons and VIP interneurons, partly overlap with those that contain ChAT (choline acetyltransferase) (Cauli *et al*, 2004), NOS and ChAT interneurons were also examined in the low-frequency IO-stimulated (4 Hz) rats and in the high-frequency TC-stimulated (30 Hz) rats. All c-Fos-immunostained sections were incubated overnight using one of the following primary antibodies: goat anti-COX-2 (1:500; Santa Cruz Biotechnology, Santa Cruz, CA, USA), rabbit anti-SOM (1:2000; Peninsula Laboratories, Belmont, CA, USA), rabbit antineuronal NOS (1:10,000; Upstate, Lake Placid, NY, USA), guinea pig anti-VIP (1:5000; Peninsula Laboratories), mouse anti-PV (1:40,000; Sigma, St Louis, MO, USA) or goat anti-ChAT (1:300; Chemicon, Temecula, CA, USA), followed by incubation with species-specific secondary antibodies (1:200, Vector Labs, Burlingame, CA). The reaction was revealed using the ABC complex (Vectastain ABC kit, Elite PK-6100, Vector Labs) and visualized using 3,3′-diaminobenzidine (DAB, kit SK-4100, Vector Labs, brown precipitate). The Sections were observed under light microscopy (Leitz Aristoplan, Leica) and digital pictures were taken (CoolPix 4500, NIKON Canada), calibrated, and edited using MetaMorph 6.1r3 (Universal Imaging, Downingtown, PA, USA) and Adobe Photoshop 7 (Adobe Systems, San Jose, CA, USA). For each rat, at least two

sections and/or two pictures/sections were used for quantification.

Tissue PO_2 (tpO_2) Measurements

We used a modified Clark-type polarographic oxygen microelectrode (OX-10, Unisense A/S, Aarhus, Denmark) with a guard cathode for tpO_2 measurements.

The field of sensitivity is a sphere of twice the tip diameter (5 to 10 μm in this study) (Thompson *et al*, 2003). The electrodes used in this study were constructed so that 90% of the response time was <1 secs, and the stirring sensitivity was nearly negligible at $<0.8\%$ Oxygen microelectrodes respond linearly to changes in oxygen concentration. Each electrode was calibrated in air-saturated and oxygen-free saline (0.9% at 37°C) before and after each experiment with reproducible oxygen measurements. Mean tpO_2 was 28.1 ± 2.3 mm Hg (mean ± s.e.m.; $n=15$), ranging from 14.0 to 37.9 mm Hg. The oxygen electrodes were stepwise, vertically inserted into the somatosensory cortex and positioned at the same cortical depth as the glass microelectrodes (300 to 600 μm). The distance between the two electrodes was ~ 200 μm. Both electrodes and the laser-Doppler flowmetry probe recorded from the same depth and were kept in the same position throughout the experiment. No linear drifts in baseline occurred during the experiments. The oxygen electrodes were connected to a high impedance Picoamperometer (PA 2000, Unisense A/S) for sensing the currents of the oxygen electrodes. Signals were A/D converted and recorded at 100 Hz (Power 1401) using the Spike 2.5 software (Cambridge Electronic Design, Cambridge, UK).

Electrophysiology

We used single-barreled glass microelectrodes, filled with 2 mol/L saline (impedance: 2 to 3 MΩ tip, 2 μm). Extracellular local field potentials (LFP) were recorded with a single electrode at a depth of 300 to 600 μm in the right sensory cortex. An Ag–AgCl ground electrode was placed in the neck muscle. The preamplified ($\times 10$) signal was A/D converted, amplified, and filtered (LFP: 1 to 1,000-Hz bandwidth), and digitally sampled using the 1401 plus hardware (CED) connected to a personal computer running the CED Spike 2.5 software. Digital sampling rates were at 5 kHz for field potentials. The LFP response amplitudes are not ideal indicators of synaptic activity, but depend on the strength of the synaptic input and the transmembrane currents that are evoked, on the distribution of the current sources and sinks and on the synchrony of the currents. The LFP response amplitudes are influenced by the position and orientation of the activated cells. Stimulation of pyramidal cells in the cerebral cortex gives rise to large LFP responses, because the dendrites are vertically organized and the cells are oriented in parallel, whereas most small interneurons do not give rise to a LFP, because of the variety in the distribution of their dendritic arborizations. Therefore, there are uncertainties in the correlation analysis between ΣLFP, blood flow, and $CMRO_2$ as presented in this study. Nevertheless, the LFP responses evoked by either TC or IO stimulation had a similar profile and were produced by the interaction of glutamate and GABA with neuronal AMPA, NMDA, and GABA receptors in adjacent cortical areas. The ΣLFP response magnitudes per stimulus rate were comparable for the two networks up to a stimulation frequency of 6 Hz, whereas at 30 and 40 Hz, it was no longer possible to identify a LFP for either network. The depression of cortical synaptic responses by IO stimulation at stimulation frequencies above 2 Hz are explained partly by subcortical adaptation at the level of the thalamus, but primarily by cortical adaptation (Chung *et al*, 2002; Martin *et al*, 2006). Adaptation was also observed for TC stimulation at comparable stimulation frequencies, but this network is not influenced by a depression at the level of the thalamus and by the decrease in LFP response amplitudes related to cortical mechanisms alone. Cortical adaptation to repeated stimuli may be explained by the prolonged duration of the inhibitory post synaptic potential (IPSP) responses, up to 100 ms by intracellular recordings, (Creutzfeldt, 1995). In addition, the membrane resistance might be short-circuited by increases in membrane conductance, but mechanisms underlying the suppression of LFP responses for rapidly repeated stimuli are incompletely understood (Creutzfeldt, 1995).

Laser-Doppler Flowmetry

Optic probes (PF 410; Perimed, Stockholm, Sweden; 780-nm wavelength, 250-μm fiber separation) were used for laser-Doppler measurements of CBF (Periflux 4001 Master, Perimed). The signal was A/D converted and recorded using the CED 1401 plus interface and the CED Spike 2.5 software (10 Hz digital sampling rate).

Calculation of $CMRO_2$

$CMRO_2$ was calculated from simultaneously obtained recordings of tpO_2 and CBF (Gjedde *et al*, 2005). The relationship between tpO_2, CBF, and $CMRO_2$ is:

$$tpO_2 = P_{50} \sqrt[h]{\frac{2C_a\,CBF}{CMRO_2}} - 1 - \frac{CMRO_2}{2L}$$

where P_{50} is the half-saturation tension of the oxygen–hemoglobin dissociation curve, h the Hill coefficient of the same dissociation curve, Ca the arterial oxygen concentration, and L the effective diffusion coefficient of oxygen in the brain tissue. The value of L was determined from baseline values of rats in similar conditions of anesthesia, in which CBF and $CMRO_2$ were reported in the literature to be 53 ml/100 g per min and 219 μmol/100 g per min (Zhu *et al*, 1998). The corresponding value of L was 4.46 μmol/100 g per min per mm Hg for standard values of P_{50} (36 mm Hg), h (2.7), and Ca (8 μmol ml^{-1}). These values were subsequently used to calculate $CMRO_2$ for each time interval, using the corresponding values of tPO_2 in mmHg and CBF in % of the baseline value. The values for each frequency were calculated by subtracting the mean baseline values (0 to 5 s before stimulation) from the evoked responses. In the following, $CMRO_2$ is presented as the

peak amplitude during stimulation. Baseline was taken as the 5 secs immediately preceding stimulation. The CBF and tpO_2 recordings were divided into bins of 1-sec duration and $CMRO_2$ was calculated as described by Gjedde *et al*, 2005.

Data Analysis and Statistics

Values are expressed as mean ± s.e.m. Student's *t*-test was used for statistical analysis. Values were considered to be statistically significant at $P<0.05$. Simultaneously recorded LFP, CBF, and tpO_2 signals were used for analysis. The LFPs were averaged and for each stimulation period, the area under curve was calculated as the sum of the time integral of the negative and the positive peaks (mV × sec). Stimulation-induced CBF and tpO_2 responses were calculated as the percentage change from baseline (5 s before stimulation). The magnitude of the response was estimated as the area under the curve above (CBF, positive tpO_2 responses) or below (negative tpO_2 responses) two s.d from baseline. Activated neurons (costained for c-Fos and one of the neuronal markers) were counted either directly under the microscope or from digital pictures taken in layers II to IV of the barrel field of the right primary somatosensory cortex (bregma levels: −2.5 to −3.5), on the side contralateral to the stimulation. The number of activated cells (c-Fos-positive) was expressed as a percentage of the total number of each population of labeled pyramidal cells or interneurons within the area of interest.

Results

Neuronal activity was increased by stimulation of the contralateral IO nerve (Nielsen and Lauritzen, 2001), or TC fibers in the homologous contralateral cortex (Olavarria *et al*, 1984). This design provided information about neurovascular and neurometabolic coupling in the same cortical area evoked by excitatory projections that target two different groups of nerve cells within the same area of the somatosensory cortex (Figure 1 and results presented below).

c-Fos Identifies Pyramidal Cells and Interneurons Activated by IO and TC Stimulation

c-Fos is a generic marker of neuronal activation considered to reflect primarily changes in afferent inputs or in external stimuli (Kovacs, 2008). The somatosensory cortex is particularly amenable to c-Fos quantification as levels are very low under basal conditions and can be induced by stimuli, such as exploration of novel environment, direct sensory stimulation, or depolarization, that increase intracellular Ca^{2+} efflux in the postsynaptic cells (Staiger *et al*, 2002). Hence, we used c-Fos immunodetection to examine whether the same types of neurons were activated by IO and TC stimulations at 4, 20, and 30 Hz in the contralateral somatosensory cortex. We found that c-Fos-immunopositive nuclei were diffusely distributed in layers II to IV with no clear barrel delineation in layer IV after low-intensity (4 Hz) IO stimulation. Both 20 and 30 Hz stimulations—similar to sham stimulation—did not induce significant levels of c-Fos expression in the somatosensory cortex (Figure 2A) despite the presence of bilateral c-Fos-positive nuclei in the thalamus, particularly in the thalamic reticular nucleus (Figure 4). TC stimulation at 4, 20, and 30 Hz evoked c-Fos immunostaining, mainly located in layers II to III, of the contralateral cortex (Figures 2A and C) (see Table 1).

Double Immunostaining Reveals the Activation of Distinct Neuronal Subpopulations

Analysis of double-immunostained cells after 4 Hz IO stimulation indicated activation of COX-2 pyramidal cells (39.3% of 926 COX-2 immunopositive pyramidal cells being c-Fos-positive) and SOM-containing interneurons (55% of 340 cells) including those that also co-localize NOS (31.5% of 130 cells). A significant proportion of PV-containing interneurons were also activated (24.9% of 251 cells) at this stimulus intensity, but there was no activation of VIP or ChAT interneurons (1 and 0% of 111 and 110 cells, respectively) (see Table 1). For TC stimulation, increases in the stimulation intensity from 4 to 30 Hz increased the proportion of activated SOM- (from 37 to 56%) and VIP- (from 0 to 18%) containing GABA interneurons, with a decreased proportion of activated COX-2 pyramidal cells (from 43 to 27%) and, prominently, PV-containing interneurons (from 44 to 2%). The results are summarized in Figure 2C (see also Table 1). Sham-stimulated rats showed no c-Fos-immunopositive cells. The data indicated that low-frequency IO stimulation, and both low- and high-frequency TC stimulations activated different cortical pyramidal cells and interneurons. We then examined how this translated into differences in synaptic activity, CBF, and $CMRO_2$ for the two networks.

Synaptic Activity and Increases in CBF

The evoked LFP responses consisted of two postsynaptic components, an initial negative potential indicating synaptic excitation (EPSP) and a positive potential indicating synaptic inhibition (IPSP) (Figure 1B). LFP responses were evoked consistently at stimulation frequencies of up to 6 Hz, but profiles and response amplitudes changed as a function of the stimulation frequency. The IPSPs were abolished at stimulation frequencies $\geq$4 Hz, and we were unable to detect any excitatory post synaptic potential (EPSP) at 30 and 40 Hz (except for the first stimulus). For stimulation frequencies of up to 6 Hz, we observed a frequency-dependent increase in synaptic activity as shown in Figure 3A, and for frequencies of up to 40 Hz we observed a linear correlation between stimulation frequency and CBF for TC stimulation, and a complex relation for IO stimulation (Figure 3B). We are aware of the limita-

tions in estimating the postsynaptic activity by LFP, as excitation of interneurons and the resulting inhibition gives rise to none or very small changes in LFP because of the functional anatomy of the interneurons. With these caveats in mind, we tested the hypothesis that the increases in CBF evoked by stimulation were triggered by excitatory synaptic activity. To this end, we correlated the ΣLFP for both networks to the respective CBF response amplitudes and observed a linear correlation for stimulation frequencies of up to 6 Hz for TC stimulation ($R^2 = 0.9846$; $P < 0.0001$) (Figure 3E), and a parabolic correlation for IO stimulation ($R^2 = 0.992$; $P < 0.0001$) (Figure 3D).

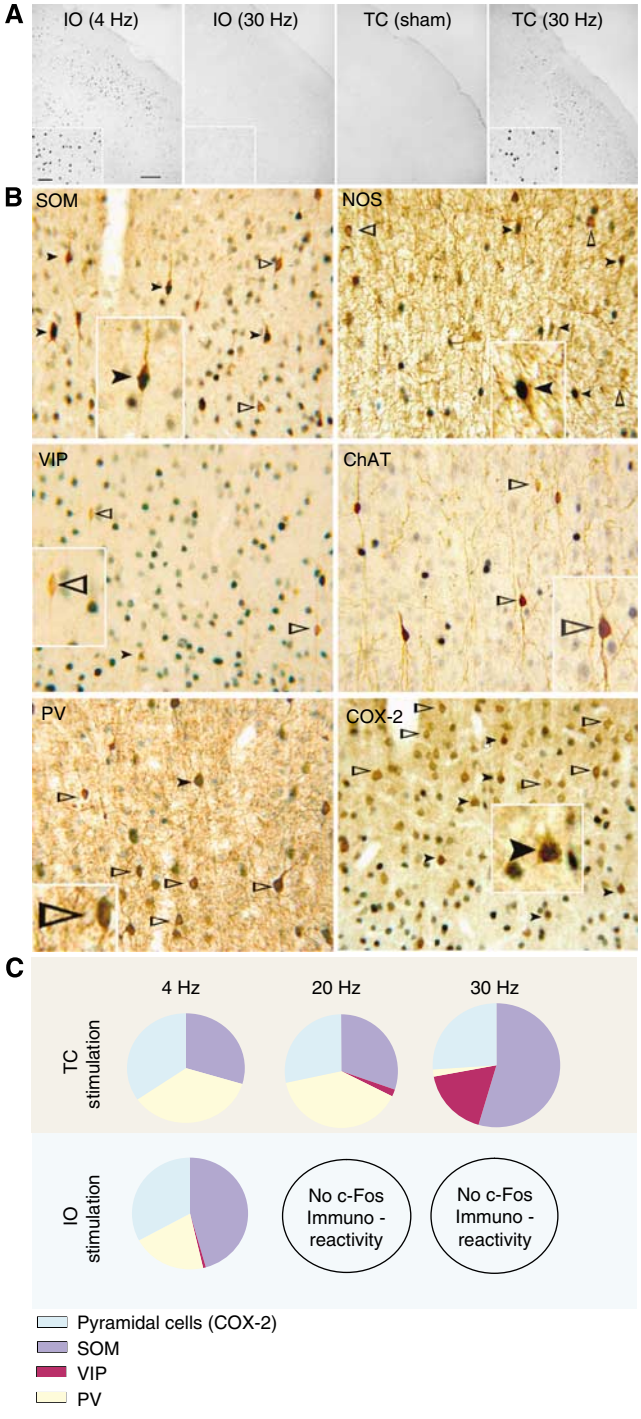

Figure 2 Specific populations of pyramidal cells and GABA interneurons are activated by low-frequency (4 Hz) IO and high-frequency (30 Hz) TC stimulations. (**A**) c-Fos immunostaining in the somatosensory cortex contralateral to IO (4 and 30 Hz) and TC (sham and 30 Hz) stimulations. Low-frequency (4 Hz) but not high-frequency (30 Hz) IO stimulation, whereas both low-frequency (not shown) and high-frequency (30 Hz) TC stimulations induced c-Fos in the target somatosensory cortex as illustrated clearly by the insets in the corresponding areas of the IO- and TC-stimulated cortex; bar = 100 μm. (**B**) In the low-frequency IO-stimulated or high-frequency TC-stimulated somatosensory cortex, several SOM- and nNOS-containing GABA interneurons were activated (c-Fos-positive nuclei, black arrowheads) as compared with that of the nonactivated (cells with c-Fos-negative nuclei, open arrowheads). Depending on the stimulus, distinct proportions of VIP- and PV-containing GABA interneurons were activated, but virtually no ChAT-containing GABA interneurons were c-Fos-positive (black arrowheads) as most of the cells did not exhibit c-Fos-positive nuclei (open arrowheads). Additionally, IO and TC simulations activated pyramidal cells, as visualized in a subset of them double-labeled for COX-2 and c-Fos (black arrowheads). Insets are larger views of selected cells in each panel. (**C**) and Table 1 shows the details on the proportion of each neuronal population activated by IO or TC stimulation.

Response Characteristics of Tissue O_2 and $CMRO_2$

IO stimulation evoked tpO_2 responses for stimulation frequencies at or below 6 Hz (Figures 1D and 3C: blue trace and green trace, respectively). The tpO_2 responses ranged from small positive deflections at 0.25 to 0.5 Hz to biphasic responses at stimulation frequencies ≥ 1 Hz (Figure 1D: blue trace). Biphasic responses consisted of an initial decrease in tpO_2 followed by a slower and longer-lasting positive response. The negative tpO_2 responses were statistically different from 0 at stimulation frequencies from 1 to 6 Hz, whereas it was absent at 30 and 40 Hz (Figures 1D and 3C: blue and green, respectively) ($n = 10$ rats). Decreases in tpO_2 began at the same time as the increase in CBF, and the subsequent development of a positive tpO_2 response paralleled the increase in CBF for all stimulation frequencies with a few-seconds delay (Figure 1D). In comparison, TC stimulation evoked reproducible tpO_2 responses for all stimulation frequencies (Figure 1F) ranging from sole increases at low frequencies (≤ 1 Hz) to biphasic responses at stimulation frequencies ≥ 1 Hz. Both the negative (Figure 3C: blue trace) and the positive (not shown) tpO_2 response area increased linearly with increasing stimulation frequency. Comparison of the time courses of the tpO_2 and CBF signals showed that the decrease in tpO_2 began at the same time as the increase in CBF (Figure 1F).

Resting $CMRO_2$ was the same for rats exposed to IO stimulation (256.9 ± 11.5 μmol/100 g per min) as

Table 1 Transcallosal (TC) and infraorbital (IO) stimulations activate different subpopulations of cortical neurons

	TC (4 Hz) (n = 4)	*TC (20 Hz)* (n = 4)	*TC (30 HZ)* (n = 4)	*IO (4 Hz)* (n = 3)	*IO (20 Hz)* (n = 3)	*IO (30 HZ)* (n = 4)
SOM	36.7 ± 4.3%	31.0 ± 2.4%	56.3 ± 9.3%	55.0 ± 3.1%	0%	0%
VIP	0%	2.2 ± 1.4%	17.7 ± 6.0%	1.0 ± 0.7%	0%	0%
(ChAT)	NT	NT	0%	0%	0%	0%
PV	43.8 ± 4.0%	39.4 ± 3.0%	1.8 ± 1.0%	24.9 ± 1.9%	0%	0%
Pyramidal COX-2	42.9 ± 6.3%	28.7 ± 1.3%	27.0 ± 6.1%	39.3 ± 3.0%	0%	0%

Number in percentage of c-Fos-immunopositive cells costained with antibodies against somatostatin (SOM), vasoactive intestinal polypeptide (VIP), parvalbumin (PV), and cycloxygenase-2 (COX-2) following TC or IO stimulation at 4, 20, and 30 Hz. (NT: not tested).

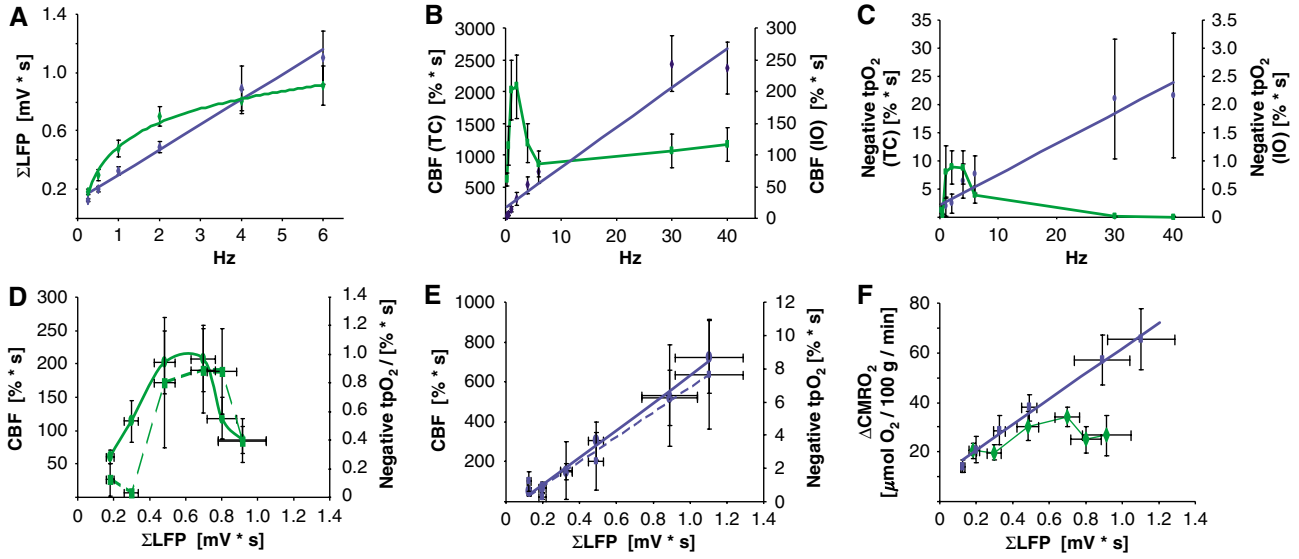

Figure 3 Neurovascular and neurometabolic coupling differ between corticocortical and thalamocortical stimulation. Stimulation-induced responses are plotted either against stimulation frequencies or synaptic activity as indicated by the summed local field potentials, ΣLFP (mV × sec). CBF responses are depicted as full lines, whereas negative tpO_2 responses are depicted as stippled lines. IO nerve stimulation is indicated by green and TC by blue. (**A**) ΣLFP, which indicates the overall level of EPSP and IPSP activities integrated over time, increased as a function of stimulation frequencies for both TC and IO stimulation. Correlation analysis revealed a linear relationship for TC stimulation ($y = 0.17x + 0.13$; $R^2 = 0.98$) and a log relation for IO stimulation ($y = 0.24 \ln(x) + 0.49$, $R^2 = 0.99$). Responses are shown only for stimulation frequencies of up to 6 Hz, as LFP responses were absent at 30 and 40 Hz. (**B**) CBF responses differed markedly between the two types of stimulation. The time-integrated hemodynamic responses were smaller for IO than for TC stimulation (see scales). The response curve for IO stimulation was a parabola with maximum CBF response at 2 Hz. The response curve for TC stimulation was linear ($y = 62.80x + 170.58$ $R^2 = 0.95$). (**C**) tpO_2 responses differed markedly between the two networks, as the area of the negative tpO_2 response was much larger for TC than for IO stimulation (note 10 × scale difference). For IO stimulation, a parabolic relation was observed between stimulation frequency and negative tpO_2. For TC stimulation, the negative area of the tpO_2 response increased monotonically with increasing stimulation frequency, which was best described as a linear relationship: $y = 0.55x + 2.10$; $R^2 = 0.95$. (**D**) Correlation of ΣLFP versus CBF and the negative tpO_2 area revealed two polynomial curves for IO nerve stimulation ($y = -1031.3x^2 + 1164.3x - 124.74$, $R^2 = 0.91$ and $y = -4.40x^2 + 5.63x - 0.95$, $R^2 = 0.77$, respectively) (**E**) For TC stimulation, the correlation of ΣLFP versus CBF and the negative tpO_2 area revealed a linear relationship ($y = 685.48x - 53.62$, $R^2 = 0.99$ and $y = 7.43x - 0.56$, $R^2 = 0.96$, respectively). (**F**) Plotting ΣLFP versus the change in $CMRO_2$, Δ $CMRO_2$, revealed a strong linear correlation for TC stimulation ($y = 51.26x + 10.60$, $R^2 = 0.99$). For IO stimulation, $\Delta CMRO_2$ was related to ΣLFP in a complex manner, the plots revealed the same polynominal curve as for CBF and negative tpO_2 area ($y = -61.04x^2 + 77.00x + 6.42$, $R^2 = 0.66$).

for TC stimulation (258.6 ± 15.8 μmol/100 g per min) (NS). The relationship between stimulation frequency and the increases in $CMRO_2$ was described by a linear relationship for IO stimulation (see Figure 5A), which included data for all frequencies of up to 40 Hz ($y = 0.3141x + 25.457$, $R^2 = 0.519$, $P = 0.04$). $CMRO_2$ was increased by 9.2% ± 1.4% at 0.25 Hz and up to 17.5% ± 4.7% at 40 Hz. The results are consistent with that of earlier data obtained in the primary somatosensory cortex using optical imaging techniques, which estimated an increase in $CMRO_2$ by up to 20% for different stimulation intensities of the whisker pad (Jones *et al*, 2001), up to 5% for stimulation of the hind paw (Sheth *et al*, 2004), and

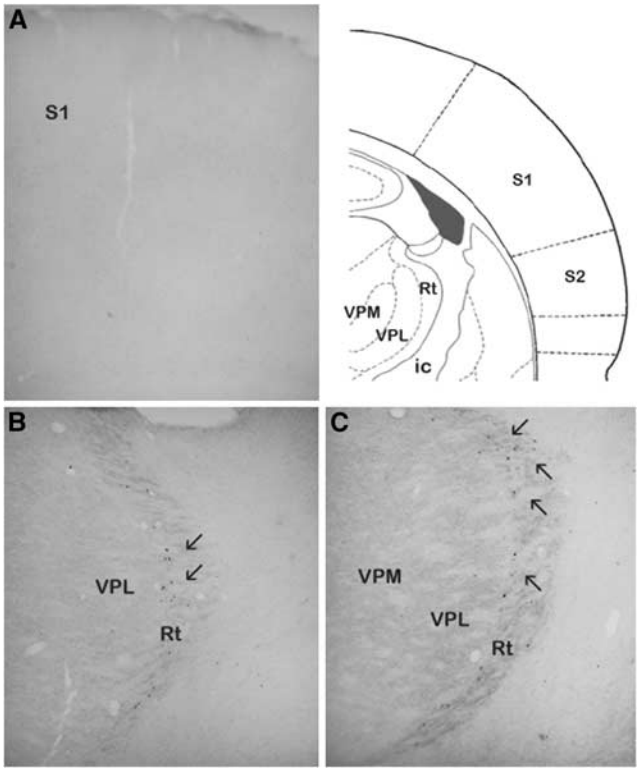

Figure 4 Thalamic activation after high frequency (20 Hz) infraorbital (IO) nerve stimulation. (**A**) c-Fos immunostaining was not detected in the primary somatosensory cortex (S1), but activation in the thalamus was evidenced, particularly in the reticular thalamic (Rt) relay nucleus, as shown at two different levels in the same rat (**B**, **C**). Activation of the ventral posteromedial (VPM) thalamic nucleus was not detected. Arrows point to c-Fos-positive nuclei in the Rt nucleus. VPL, ventral posterolateral nucleus; ic, internal capsule; S2, secondary somatosensory cortex.

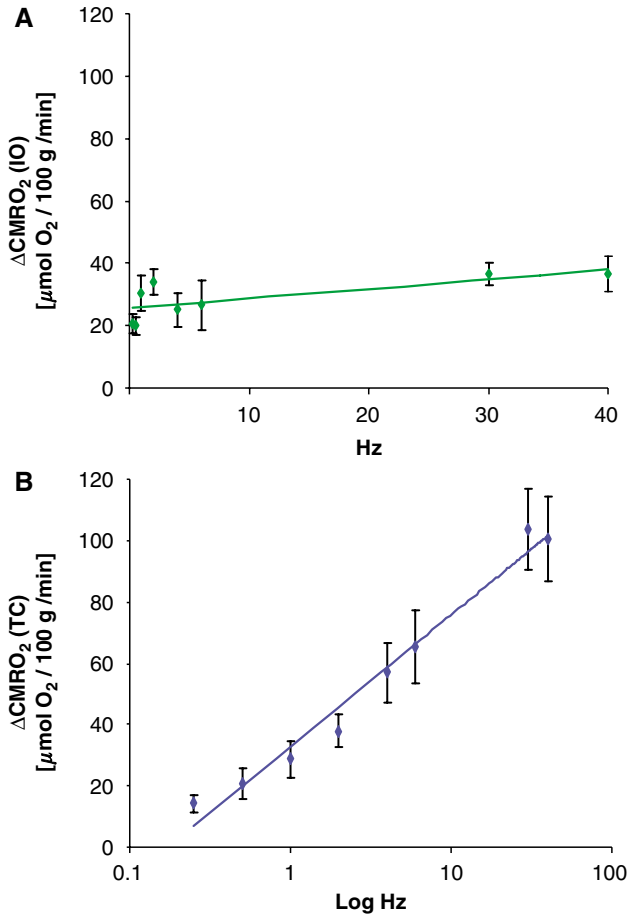

Figure 5 Frequency-dependency of $CMRO_2$ dynamics. Cortical oxygen consumption ($CMRO_2$) was calculated from the simultaneous measurements of CBF and tpO_2 for the whole period of stimulation. All values are given as mean ± s.e.m. Findings were described by a linear increase of $CMRO_2$ for IO stimulation (**A**) ($y = 0.3141x + 25.457$, $R^2 = 0.519$) ($n = 10$) and a logarithmic increase of $CMRO_2$ for TC stimulation (**B**) ($y = 18.66 \ln(x) + 32.78$; $R^2 = 0.98$) ($n = 6$).

2% for stimulation of single whiskers (Weber *et al*, 2004). For TC stimulation, the relationship was logarithmic (see Figure 5B) ($R^2 = 0.9768$; $P = 0.0001$). $CMRO_2$ increased by 5.2 ± 1.1% at 0.25 Hz and up to 37.1 ± 6.4% at 40 Hz. There are only few data available for metabolic and hemodynamic changes after TC stimulation in the literature, but our data are consistent with that of earlier studies in the motor cortex showing strongly localized, stimulus frequency-dependent (0.1 to 1.0 Hz) increases in glucose consumption (Weber *et al*, 2002), and a positive BOLD signal increases of 3.7% (300 Hz) (Austin *et al*, 2003).

Neurovascular and Neurometabolic Coupling Differ Importantly Between the Two Networks

Finally, we assessed the neurometabolic and neurovascular coupling in the two networks by the correlation of ΣLFP to CBF and the negative tpO_2 area for the two types of stimulation. For IO stimulation, the relation was best described by a parabola; the negative tpO_2 area and CBF increased, saturated, and decreased again corresponding to a stimulation frequency of 4 Hz (Figure 3D). In comparison, for TC stimulation (Figure 3E), the relations between ΣLFP versus the negative tpO_2 area (stippled line) and CBF (solid line) were well described by linear correlations ($R^2 = 0.9639$; $P = 0.0005$; $R^2 = 0.992$; $P = 0.0001$, respectively). Similarly, for TC stimulation, the correlation between ΣLFP versus $CMRO_2$ was linear ($R^2 = 0.9914$; $P = 0.0001$), whereas the relation for IO stimulation was best described as a parabola (Figure 3F). The results suggest that local variations in the coupling between synaptic activity and $CMRO_2$ reflect increased activity within the targeted network, the latter being a function of the afferent input.

Discussion

The BOLD signal has been thought to be independent of the type of information processing. In this study,

we imply that the amplitude of BOLD signals will depend critically on the type of input that activates a cortical area and hence, on the neurons involved in the local processing of the incoming afferent information. We show that the neurovascular and neurometabolic coupling responses to thalamocortical and corticocortical stimulation concurred with the activation of specific networks of principal cells, including COX-2 expressing pyramidal cells and GABAergic interneurons that differ with regard to the vasoactive compound they contain, and that the identity of the activated cells varied with the stimulus frequency. These findings highlight the contributions of both excitatory pyramidal cells and inhibitory interneurons in the hemodynamic and metabolic responses to increased neuronal activity and, furthermore, they show that the neuronal network activation is both stimulus- and frequency-dependent. We have conducted IO and TC stimulation experiments in the same animals as well. The problem with this approach is that the stimulation of one network influences the subsequent activity evoked in the other. This could be because of the activation of NMDA receptors and hence, neuronal Ca^{2+} changes at the high stimulation intensities. For these reasons, we only report from different series of animals in this paper.

IO and TC stimulation trigger activity in multisynaptic pathways; the thalamocortical input to layer IV rapidly spreads to neurons in layers II and III (Armstrong-James *et al*, 1992), whereas activity of the TC projections spreads to neurons in all layers of the cortex, except layer IV (Shepherd *et al*, 2005; Petreanu *et al*, 2007). Therefore, the differences in neurovascular and neurometabolic coupling are likely not explained by the differences in the number of intracortical synapses being activated. Our study was performed in anesthetized rats, and it is possible that anesthesia alters the function of specific pathways and synapses to a different extent, as discussed in the following.

The observed differences in neurometabolic and vascular coupling between the two afferent pathways were supported by the c-Fos data. For low-intensity (4 Hz) IO stimulation, activation of COX-2 pyramidal cells and GABA interneurons that contain SOM (±NOS) and PV concurred with an earlier report of both excitatory and inhibitory neurons expressing c-Fos in the somatosensory cortex after exploration of a novel environment (Staiger *et al*, 2002). However, the lack of c-Fos-positive VIP interneurons after IO stimulation as compared with overnight exploration of a new environment is unclear, but it is most likely that differences in the status of the animals (anesthetized versus freely moving) and duration of the stimulus (20 mins versus overnight) are key determinants of the neuronal populations that respond to these comparable, albeit different, stimuli. IO stimulation at high intensity (20 and 30 Hz) resulted in no detectable activation of cortical neurons using c-Fos as a marker, a finding that correlated with the absence of tpO_2 dip and LFP responses, and the IO stimulation plots of synaptic activity with CBF and $CMRO_2$ displaying bell-shaped curves with very low responses at 30 Hz. They also agree with the reported decrement in the spiking rate of layers III and IV barrel neurons with increased stimulus frequency (Melzer *et al*, 2006). Our findings can well be explained by the frequency-dependent adaptation of cortical neurons, which occurs rapidly such that above 1 Hz, many cortical neurons cease firing after the first few deflections (Melzer *et al*, 2006). Although the strength of the adaptation observed here and in other studies can be attributed, in part, to the depth of the anesthesia (Chung *et al*, 2002), similar modulation of thalamocortical synapses has been reported in the awake state (Swadlow and Gusev, 2001). This contrasts with neurons in the ventroposterior medial nucleus (VPM) of the thalamus, the main sensory input to the barrel cortex, which adapted modestly and only at higher frequencies (>4 Hz) (Chung *et al*, 2002). Our finding of c-Fos-immunopositive cells in the reticular thalamic relay nucleus (Rt) in the same rats that showed no cortical activation at high frequency stimulation, confirmed that pathway activation did occur. Furthermore, they illustrated, in the live animals, the importance of Rt neurons in modulating and gating the activity of VPM neurons (Hartings *et al*, 2000), and the high frequency-dependent adaptation of cortical neurons (Swadlow and Gusev, 2001).

During TC stimulation, a frequency-dependent response for cortical neuron activation was observed between 4 and 30 Hz. Stimulation at 4 Hz activated both excitatory COX-2-expressing pyramidal cells (Yamagata *et al*, 1993) and specific subtypes of inhibitory GABA interneurons that contain PV and SOM; a subset of the latter are also known to contain NOS (Kubota *et al*, 1994). At 30 Hz, a larger fraction of SOM interneurons were activated together with a subset of VIP interneurons, but there was a silencing of those containing PV. These results suggest a recruitment of activated neurons as a function of stimulus intensity. However, they also point to specific neurons being unable to sustain activation at such high intensities, because of differences in their respective resting potential and input resistance (Kawaguchi and Kubota, 1993) or, alternatively, being inhibited by other networks of activated inhibitory interneurons (Hestrin and Galarreta, 2005). The latter possibility seems most likely, because PV neurons can sustain a high frequency stimulation and show little or no frequency adaptation (Kawaguchi and Kubota, 1993; Cauli *et al*, 1997). Interestingly, SOM interneurons, which exhibited the highest activation at 30 Hz, correspond to Martinotti interneurons whose activity has been shown to correlate with the inhibition of the fast-spiking PV-containing interneuron network (Beierlein *et al*, 2000). In addition, the silencing of PV interneurons at high frequency could be explained by the newly recruited VIP interneurons, which target PV neurons in the barrel cortex on which they

are believed to exert an inhibitory effect (David *et al*, 2007). Together, these anatomic findings suggest that the *in vivo* changes in CBF, tpO2, and $CMRO_2$ responses, which are their highest at 30 Hz TC stimulation, are primarily driven by increased activity in pyramidal cells and SOM (±NOS) interneurons. Involvement of NOS and COX derivatives in the evoked CBF responses to these two networks is consistent with studies showing that increases in CBF produced by TC stimulation are blocked by NOS and COX inhibitors (Hoffmeyer *et al*, 2007), and that COX-2- and NOS-derived vasoactive metabolites are involved in the neurovascular coupling response to whisker stimulation (Niwa *et al*, 2000; Gotoh *et al*, 2001).

The results of our study emphasize the contribution of GABA interneurons in the neurovascular coupling response to distinct afferent pathways (Cauli *et al*, 2004; Kocharyan *et al*, 2008). Changes in $CMRO_2$ evoked by corticocortical stimulation correlated linearly to ΣLFP, whereas for thalamocortical stimulation, $CMRO_2$ increased frequency-dependently up to 2 Hz and declined at higher frequencies. This indicates that the increases in CBF and $CMRO_2$ were far more pronounced for corticocortical than for thalamocortical stimulation for the same level of stimulus frequency, and suggests that the neurometabolic and neurovascular coupling responses differ among networks targeting the same small cortical region. This is not surprising, as CBF and metabolic responses within a given region of the brain reflect the combined activities in mixtures of cells and synapses that include both excitatory and inhibitory processes, which differ in their capacity to synthesize and release vasoactive molecules or induce their release from perivascular astrocytes. Moreover, the subsets of recruited neurons may change as a function of both the afferent pathway and the stimulation frequency. Therefore, inputs to the same region of the brain that contains a variety of neurons and synapses do not have equal effects on blood flow and metabolism, which would also be reflected in the fMRI BOLD signals recorded in activation studies. Although synaptic inhibition *per se* may give rise to negative BOLD signals (Shmuel *et al*, 2006; Lauritzen, 2005), our data show that activation of pyramidal cells and inhibitory interneurons give rise to an overall increase in the CBF response, and in consequence, to a positive BOLD responses. Our finding points to a complex interaction between cortical inhibitory networks, pyramidal cell activity, and hemodynamic responses. We suggest that variations in response amplitudes and phase of functional neuroimaging signals, such as the BOLD signal depend on the properties of the activated networks and, hence, on the type of activated nerve cells.

Acknowledgements

The authors thank David Attwell for his valuable comments on this paper. This study was supported by the Lundbeck Foundation Centre for Neurovascular Signaling (LUCENS), the NOVO Nordisk Foundation and the Danish Medical Research Council, and by a Grant (MOP-84209 to EH) from the Canadian Institutes of Health Research (CIHR).

References

Armstrong-James M, Fox K, Das-Gupta A (1992) Flow of excitation within rat barrel cortex on striking a single vibrissa. *J Neurophysiol* 68:1345–58

Armstrong-James M, Welker E, Callahan CA (1993) The contribution of NMDA and non-NMDA receptors to fast and slow transmission of sensory information in the rat SI barrel cortex. *J Neurosci* 13:2149–60

Austin VC, Blamire AM, Grieve SM, O'Neill MJ, Styles P, Matthews PM, Sibson NR (2003) Differences in the BOLD fMRI response to direct and indirect cortical stimulation in the rat. *Magn Reson Med* 49:838–47

Beierlein M, Gibson JR, Connors BW (2000) A network of electrically coupled interneurons drives synchronized inhibition in neocortex. *Nat Neurosci* 3:904–10

Cauli B, Audinat E, Lambolez B, Angulo MC, Ropert N, Tsuzuki K, Hestrin S, Rossier J (1997) Molecular and physiological diversity of cortical nonpyramidal cells. *J Neurosci* 17:3894–906

Cauli B, Tong XK, Rancillac A, Serluca N, Lambolez B, Rossier J, Hamel E (2004) Cortical GABA interneurons in neurovascular coupling: relays for subcortical vasoactive pathways. *J Neurosci* 24:8940–9

Chung S, Li X, Nelson SB (2002) Short-term depression at thalamocortical synapses contributes to rapid adaptation of cortical sensory responses in vivo. *Neuron* 34:437–46

Conti F, Manzoni T (1994) The neurotransmitters and postsynaptic actions of callosally projecting neurons. *Behav Brain Res* 64:37–53

Creutzfeldt OD (1995) Spontaneous and evoked cortical potentials and related neuronal events. In: *Cortex cerebri*. Oxford University Press, 165–220

David C, Schleicher A, Zuschratter W, Staiger JF (2007) The innervation of parvalbumin-containing interneurons by VIP-immunopositive interneurons in the primary somatosensory cortex of the adult rat. *Eur J Neurosci* 25: 2329–40

Gjedde A, Johannsen P, Cold GE, Ostergaard L (2005) Cerebral metabolic response to low blood flow: possible role of cytochrome oxidase inhibition. *J Cereb Blood Flow Metab* 25:1183–96

Gotoh J, Kuang TY, Nakao Y, Cohen DM, Melzer P, Itoh Y, Pak H, Pettigrew K, Sokoloff L (2001) Regional differences in mechanisms of cerebral circulatory response to neuronal activation. *Am J Physiol Heart Circ Physiol* 280:H821–9

Hartings JA, Temereanca S, Simons DJ (2000) High responsiveness and direction sensitivity of neurons in the rat thalamic reticular nucleus to vibrissa deflections. *J Neurophysiol* 83:2791–801

Hestrin S, Galarreta M (2005) Synchronous versus asynchronous transmitter release: a tale of two types of inhibitory neurons. *Nat Neurosci* 8:1283–4

Hoffmeyer HW, Enager P, Thomsen KJ, Lauritzen MJ (2007) Nonlinear neurovascular coupling in rat sensory cortex by activation of transcallosal fibers. *J Cereb Blood Flow Metab* 27:575–87

Jones M, Berwick J, Johnston D, Mayhew J (2001) Concurrent optical imaging spectroscopy and laser-Doppler flowmetry: the relationship between blood flow, oxygenation, and volume in rodent barrel cortex. *Neuroimage* 13:1002–15

Kadekaro M, Crane AM, Sokoloff L (1985) Differential effects of electrical stimulation of sciatic nerve on metabolic activity in spinal cord and dorsal root ganglion in the rat. *Proc Natl Acad Sci USA* 82:6010–3

Kawaguchi Y, Kubota Y (1993) Correlation of physiological subgroupings of nonpyramidal cells with parvalbumin- and calbindinD28k-immunoreactive neurons in layer V of rat frontal cortex. *J Neurophysiol* 70:387–96

Kocharyan A, Fernandes P, Tong XK, Vaucher E, Hamel E (2008) Specific subtypes of cortical GABA interneurons contribute to the neurovascular coupling response to basal forebrain stimulation. *J Cereb Blood Flow Metab* 28:221–31

Kovacs KJ (2008) Measurement of immediate-early gene activation- c-fos and beyond. *J Neuroendocrinol* 20: 665–72

Kubota Y, Hattori R, Yui Y (1994) Three distinct subpopulations of GABAergic neurons in rat frontal agranular cortex. *Brain Res* 649:159–73

Lauritzen M (2005) Opinion: Reading vascular changes in brain imaging: is dendritic calcium the key? *Nat Rev Neurosci* 6:77–85

Logothetis NK, Pauls J, Augath M, Trinath T, Oeltermann A (2001) Neurophysiological investigation of the basis of the fMRI signal. *Nature* 412:150–7

Martin C, Martindale J, Berwick J, Mayhew J (2006) Investigating neural-hemodynamic coupling and the hemodynamic response function in the awake rat. *Neuroimage* 32:33–48

Melzer P, Sachdev RN, Jenkinson N, Ebner FF (2006) Stimulus frequency processing in awake rat barrel cortex. *J Neurosci* 26:12198–205

Nielsen A, Lauritzen M (2001) Coupling and uncoupling of activity-dependent increases of neuronal activity and blood flow in rat somatosensory cortex. *J Physiol* 533: 773–85

Niwa K, Araki E, Morham SG, Ross ME, Iadecola C (2000) Cyclooxygenase-2 contributes to functional hyperemia in whisker-barrel cortex. *J Neurosci* 20: 763–70

Olavarria J, Van Sluyters RC, Killackey HP (1984) Evidence for the complementary organization of callosal and thalamic connections within rat somatosensory cortex 48. *Brain Res* 291:364–8

Petreanu L, Huber D, Sobczyk A, Svoboda K (2007) Channelrhodopsin-2-assisted circuit mapping of long-range callosal projections. *Nat Neurosci* 10:663–8

Raichle ME, Mintun MA (2006) Brain work and brain imaging. *Annu Rev Neurosci* 29:449–76

Schwartz WJ, Smith CB, Davidsen L, Savaki H, Sokoloff L, Mata M, Fink DJ, Gainer H (1979) Metabolic mapping of functional activity in the hypothalamo-neurohypophysial system of the rat. *Science* 205:723–5

Shepherd GMG, Stepanyants A, Bureau I, Chklovskii D, Svoboda K (2005) Geometric and functional organization of cortical circuits. *Nat Neurosci* 8:782–90

Sheth SA, Nemoto M, Guiou M, Walker M, Pouratian N, Toga AW (2004) Linear and nonlinear relationships between neuronal activity, oxygen metabolism, and hemodynamic responses. *Neuron* 42:347–55

Shmuel A, Augath M, Oeltermann A, Logothetis NK (2006) Negative functional MRI response correlates with decreases in neuronal activity in monkey visual area V1. *Nat Neurosci* 9:569–77

Sokoloff L (1999) Energetics of functional activation in neural tissues. *Neurochem Res* 24:321–9

Staiger JF, Masanneck C, Bisler S, Schleicher A, Zuschratter W, Zilles K (2002) Excitatory and inhibitory neurons express c-Fos in barrel-related columns after exploration of a novel environment. *Neuroscience* 109:687–99

Swadlow HA, Gusev AG (2001) The impact of 'bursting' thalamic impulses at a neocortical synapse. *Nat Neurosci* 4:402–8

Thompson JK, Peterson MR, Freeman RD (2003) Single-neuron activity and tissue oxygenation in the cerebral cortex. *Science* 299:1070–2

Weber B, Burger C, Wyss MT, von Schulthess GK, Scheffold F, Buck A (2004) Optical imaging of the spatiotemporal dynamics of cerebral blood flow and oxidative metabolism in the rat barrel cortex. *Eur J Neurosci* 20:2664–70

Weber B, Fouad K, Burger C, Buck A (2002) White matter glucose metabolism during intracortical electrostimulation: a quantitative [F-18]fluorodeoxyglucose autoradiography study in the rat. *Neuroimage* 16:993–8

Wise SP, Jones EG (1976) The organization and postnatal development of the commissural projection of the rat somatic sensory cortex. *J Comp Neurol* 168:313–43

Woolsey TA, Rovainen C (1991) Whisker barrels: a model for direct observation of changes in cerebral microcirculation with neuronal activity. In: *Brain Work and Mental Activity* (Lassen NA, Ingvar DH, Raichle ME, Friberg L, eds), Copenhagen: Mungsgaard, 189–98

Yamagata K, Andreasson KI, Kaufmann WE, Barnes CA, Worley PF (1993) Expression of a mitogen-inducible cyclooxygenase in brain neurons: regulation by synaptic activity and glucocorticoids. *Neuron* 11:371–86

Zhu XH, Kim SG, Andersen P, Ogawa S, Ugurbil K, Chen W (1998) Simultaneous oxygenation and perfusion imaging study of functional activity in primary visual cortex at different visual stimulation frequency: quantitative correlation between BOLD and CBF changes. *Magn Reson Med* 40:703–11